STEM CELLS®

REGENERATIVE MEDICINE

Age-Related Changes in Speed and Mechanism of Adult Skeletal Muscle Stem Cell Migration

HENRY COLLINS-HOOPER,[a] THOMAS E. WOOLLEY,[b] LOUISE DYSON,[b] ANAND PATEL,[a] PAUL POTTER,[c] RUTH E. BAKER,[b] EAMONN A. GAFFNEY,[b] PHILIP K. MAINI,[b] PHILIP R. DASH,[a] KETAN PATEL[a]

[a]School of Biological Sciences, University of Reading, Reading, United Kingdom; [b]Centre for Mathematical Biology, Mathematical Institute, University of Oxford, Oxford, United Kingdom; [c]MRC Harwell, Oxfordshire, United Kingdom

Key Words. Ageing • Bleb • Migration • Satellite • Amoeboid • Stem • Cell • Skeletal • Muscle

ABSTRACT

Skeletal muscle undergoes a progressive age-related loss in mass and function. Preservation of muscle mass depends in part on satellite cells, the resident stem cells of skeletal muscle. Reduced satellite cell function may contribute to the age-associated decrease in muscle mass. Here, we focused on characterizing the effect of age on satellite cell migration. We report that aged satellite cells migrate at less than half the speed of young cells. In addition, aged cells show abnormal membrane extension and retraction characteristics required for amoeboid-based cell migration. Aged satellite cells displayed low levels of integrin expression. By deploying a mathematical model approach to investigate mechanism of migration, we have found that young satellite cells move in a random "memoryless" manner, whereas old cells demonstrate superdiffusive tendencies. Most importantly, we show that nitric oxide, a key regulator of cell migration, reversed the loss in migration speed and reinstated the unbiased mechanism of movement in aged satellite cells. Finally, we found that although hepatocyte growth factor increased the rate of aged satellite cell movement, it did not restore the memoryless migration characteristics displayed in young cells. Our study shows that satellite cell migration, a key component of skeletal muscle regeneration, is compromised during aging. However, we propose clinically approved drugs could be used to overcome these detrimental changes. STEM CELLS *2012;30:1182–1195*

Disclosure of potential conflicts of interest is found at the end of this article.

INTRODUCTION

The increase in the longevity of individuals in Western societies will present considerable challenges to the healthcare and economic systems of developed countries as they care for people whose body functions undergo age-related deterioration. Changes in the structure and function of skeletal muscle with regards to ageing have been extensively studied not only in animal models but also in humans. Old age is associated with a progressive loss of skeletal muscle mass, a process called sarcopenia. Age-related muscle loss leads to lack of muscle strength, resulting in reduced posture and mobility and an increased risk of falls, all of which contribute to a decrease in quality of life [1]. In humans, sarcopenia first becomes evident at middle age. Large population studies have reported that more than 20% of 60- to 70-year olds have sarcopenia and that the number reaches 50% in those who are more than 75 years of age. [2].

Aged skeletal muscle undergoes a progressive reduction in the cross-sectional area of muscle fibers [3], selective loss of fast glycolytic fibers [4], and increase in muscle connective tissue [5]. At the subcellular level, aged muscle fibers display an increased level of mitochondrial abnormalities and susceptibility to apoptosis [6, 7]. Myofibers from aged muscle show a reduction in force generation and are more susceptible to contraction-induced injury.

Elegant studies performed by Gutmann and Carlson have shown that aged skeletal muscle can regenerate, but the rate of regeneration diminishes over time [8]. The repair and maintenance of skeletal muscle is carried out by a resident stem cell population known as satellite cells that are located beneath the basal lamina that surrounds each myofiber. Satellite cells are maintained in a metabolically quiescent state in undamaged muscle. Upon injury, satellite cells undergo a process of activation that involves extensive changes in gene expression. Activated cells subsequently divide to form a pool of myoblasts that then differentiate to form myotubes,

Author contributions: H.C.: collection and/or assembly of data, data analysis and interpretation, manuscript writing, and final approval of manuscript; T.E.W. and L.D.: data analysis and interpretation, manuscript writing, and final approval of manuscript; A.P.: collection and/or assembly of data and final approval of manuscript; P.P.: provision of study material or patients and final approval of manuscript; R.E.B., E.A.G., and P.K.M.: data analysis and interpretation and final approval of manuscript; P.R.D.: conception and design, data analysis and interpretation, manuscript writing, and final approval of manuscript; K. P.: conception and design, financial support, data analysis and interpretation, manuscript writing, and final approval of manuscript.

Correspondence: Ketan Patel, Ph.D., School Biological Sciences, Hopkins Building, University of Reading, Whiteknights, Reading, Berkshire, RG6 6UB, U.K.. Telephone: +44-0118-378-8079; Fax: 0044 118 378 6642; e-mail: ketan.patel@reading.ac.uk Received September 28, 2011; accepted for publication February 6, 2012; first published online in STEM CELLS *EXPRESS* March 30, 2012. 1066-5099/2012/$30.00/0 doi: 10.1002/stem.1088

replacing or supplementing existing muscle. Satellite cells from aged muscle display a lag in the initiation of proliferation following their isolation as well as decreased capacity to generate progeny, indicative of compromised activation and proliferation [9].

A much neglected feature of regeneration is the necessity for satellite cells to migrate to the lesion focus in order to carry out cellular tissue repair. Recent work using high-resolution in vivo imaging of muscle has shown the directional movement of satellite cells to the site of myofiber damage [10]. Furthermore, matrix metalloproteinase, which promotes muscle cell migration and differentiation, has been shown to significantly increase the size of myoblast engraftment territory in a regenerating model [11]. The importance of satellite cell migration for tissue regeneration is evident from animal models and human trials using myoblast injection aimed at restoring muscle function [12–14]. The failure of these studies was largely due to the fact that cells rarely moved from the point of injection and did not display the requisite whole muscle dispersal. Using time-lapse microscopy, we and others examined the movement of satellite cells localized on muscle fibers and have shown a number of unexpected features, including the ability of cells to rapidly change direction, to migrate as clusters of cells, and jump from one fiber to another [15, 16].

Migration has been traditionally explained by the force generated by structures called lamellipodia that form at the leading edge of the cells and the retraction of the cell at the rear. However, a wealth of data has recently emerged showing that cells can move using a novel mechanism called blebbing or amoeboid-based movement mediated by extension of plasma membrane protrusions—or blebs—into the extracellular matrix driven by local hydrodynamic changes in cytosolic pressure [17, 18]. We demonstrated that satellite cells move on their in vivo substrate using an amoeboid or bleb-dependent mechanism rather than using lamellipodia [15]. In addition, we also showed that the ability of satellite cells to form blebs and migrate was dependent on nitric oxide (NO), a potent signaling molecule that regulates cell movement in numerous biological systems including endothelial, epithelial, and trophoblast cells [15].

In this study, we have compared migration characteristics of satellite cells localized on muscle fibers isolated from young (4 months) and aged mice (24 months) using time-lapse microscopy. We report that satellite cells from aged animals migrate significantly slower than young satellite cells. By comparing statistics from the tracked data to those derived from Fickian diffusion, we characterized the migration of satellite cells along the fibers from the two age groups. This provided us with evidence that the young cells move with diffusive characteristics while old cells display superdiffusive traits, indicating that satellite cells from old muscle move in a fundamentally different way. We show that the addition of exogenous NO reverses both the speed deficit of old satellite cells and their movement characteristics so that they move in the manner of young cells. Interestingly, we found that hepatocyte growth factor (HGF), a proposed downstream target of NO-mediated signaling rescued the speed deficit of aged satellite cells but was unable to reinstate the memoryless migration characteristics of young cells.

METHODS

Single Myofiber Culture

Myofibers were isolated from the extensor digitorum longus (EDL) muscle of eight male 4-month-old (young) and eight male 24-month-old (old) C57Bl6 mice as described previously [19]. Briefly, an undamaged EDL muscle was dissected with both tendons intact, and single fibers were liberated through digestion with (0.2%) type I collagenase in Dulbecco's modified Eagle's medium (DMEM) at 37°C under 5% CO_2. Using tapered glass pipettes, single fibers were plated out in floating culture wells containing DMEM supplemented with 10% horse serum and 0.5% chick embryo extract. When required, the NO donor (Z)-1-[N-(3-aminopropyl)-N-(n-propyl)amino]diazen-1-ium-1,2-diolate-(PAPA-NONOate) (100 μM) or HGF (20–100 ng/ml, R&D Systems) was added to myofiber culture media 24 hours after culture initiation.

Time-Lapse Microscopy

Myofiber cultures were monitored using phase-contrast microscope systems that harbor controlled-environment chambers maintained at 37°C, supplemented with 5% CO_2. Time-lapse video was taken at rate of one frame every 15 minutes for periods of up to 24 hours for satellite cells using a ×10 objective, a previously well-studied time course of satellite cell progression following skeletal muscle injury [19, 20]. In a separate analysis, high-power time-lapse microscopy using a ×100 objective was carried out, enabling the visualization of cell surface blebbing on single satellite cells. For such analysis, cells were cultured for 24–48 hours, then selected, and subsequently filmed at a rate of one frame per 2 seconds.

Immunocytochemistry

Immunocytochemistry of satellite cells on single myofibers was carried out as described previously described [19]. Briefly, fibers were fixed in 4% paraformaldehyde in phosphate buffered saline-(PBS) (PFA) for 10 minutes and washed three times in PBS. Myofibers were permeabilized in a solution of 20 mM HEPES, 300 mM sucrose, 50 mM NaCl, 3 mM $MgCl_2$, and 0.5% Triton X-100 (pH 7) at 4°C for 15 minutes and incubated in blocking wash buffer (5% newborn calf serum in PBS containing 0.01% Triton X-100) for 30 minutes prior to antibody incubation. Antibodies were diluted and preblocked in wash buffer for 30 minutes prior to addition to the myofibers. Primary antibodies used were: polyclonal rabbit anti-laminin (Sigma L-9393, 1:200), monoclonal mouse anti-Pax7 (Developmental Studies Hybridoma Bank, 1:1), polyclonal rabbit-anti-MyoD (Santa Cruz Biotechnology, 1:200), polyclonal rabbit-anti-myogenin (Santa Cruz Biotechnology, 1:200), eNOS rabbit polyclonal IgG (Santa Cruz Biotechnology, Santa Cruz, USA, http://www.scbt.com/ [sc-654], 1:200), anti-integrin α6 rat monoclonal (Abcam [ab105669], 1:200), integrin β1 mouse monoclonal (Santa Cruz, Cambridge UK, http://www.abcam.com/ Biotechnology [sc-9970], 1:200), and anti-integrin α7 rabbit (1:200) (antibody was a gift from Professor Uli Mayer). All primary antibodies were incubated overnight at 4°C. Primary antibodies were visualized using the following secondary antibodies: Alexa Fluor goat anti-mouse 488 (Molecular Probes, Grand Island, NY, USA, www.invitrogen.com, A11029), Alexa Fluor goat anti-rabbit 633 (Molecular Probes, A21071), and fluorescein rabbit anti-rat IgG (Vector Laboratories (FI-4000), 1:200). Secondary antibodies were used at 1:200 and incubated at room temperature for 45 minutes. All myofibers were mounted in fluorescent mounting medium (DAKO) containing 5 μg/ml 4',6-diamidino-2-phenylindole-(DAPI) for nuclear visualization.

Fluorescence Microscopy

Mounted myofibers were analyzed using a Zeiss Axioscope fluorescent microscope, and images were captured using an Axiocam digital camera system and analyzed using Axiovision image analysis software (version 4.7).

Scanning Electron Microscopy

Single myofibers were fixed in 4% PFA for 10 minutes. Myofibers were dehydrated through 30, 50, 70, 80, 90, and 100% ethanol solutions (15 minutes for each step) and transferred to a critical point drier (Balzers CPD 030—using liquid carbon

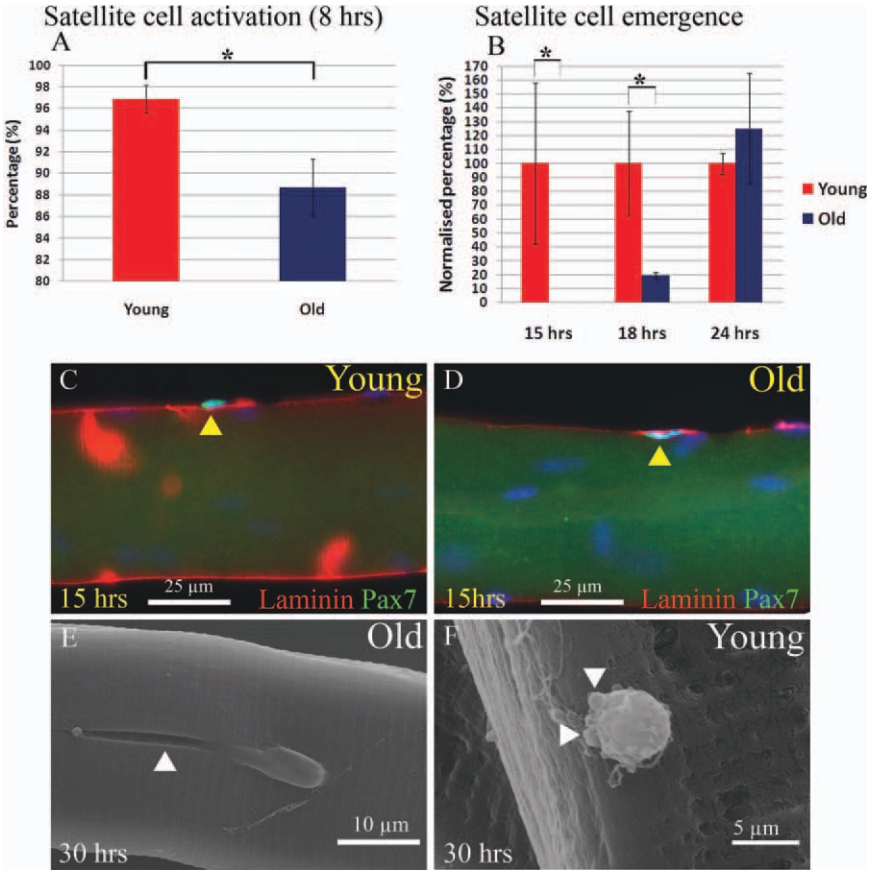

Figure 1. Delayed activation and emergence of aged satellite cells compared to young satellite cells. **(A):** Significantly fewer satellite cells from aged animals expressed MyoD (88%), a marker of activation, 8 hours after fiber isolation compared to those on young muscle fibers (96%) (*, $p < .001$). **(B):** Emergence of satellite cells (identified through expression of Pax7 taking a position on top of basal lamina containing laminin) from young and aged fibers. The number of emerging satellite cells was first calculated as a proportion of satellite cells in suprabasal position relative to all satellite cells. The percentage at each time point was set to 100 for the young fibers, and the aged cell number compared to this figure. Young fibers contained significantly more satellite cells in suprabasal positions after 15 hours and 18 hours compared to aged fibers (*, $p < .001$). **(C):** Immunocytochemical staining of a single young myofiber using antibodies against laminin and Pax7 to show the suprabasal position of the satellite cell (arrowhead) at 15 hours. **(D):** Pax7 expressing aged satellite cell (arrowhead) is still under the basal lamina in old muscle fibers at 15 hours. **(E):** Scanning electron micrograph of old muscle fiber 30 hours after culture. The satellite cell emerges with a smooth surface leaving a scar in the basal lamina (arrowhead). **(F):** Scanning electron micrograph of young muscle fibers 30 hours after culture. The satellite cell displays numerous cytoplasmic protrusions or blebs (arrowhead).

dioxide). Dried myofibers were transferred to scanning electron microscopy (SEM) chucks using microforceps under a light microscope. Thereafter, myofibers were gold-coated using an Edwards S150B sputter-coater and examined using a FEI 600F scanning electron microscope aided by analysis software for image collection.

Image and Movie Analysis

All image analysis was carried out using freeware package ImageJ (version 1.4.3). Satellite cells were individually manually tracked using the plugin MTrackJ, and bleb dynamics were quantified using ImageJ. Bleb number was quantified manually on SEM images of cells using Adobe Photoshop version CS2, only SEM images of whole cells were used for quantification. Satellite cell differentiation profiles following differing culture conditions were manually assessed using quantification of live images through the Zeiss axioscope and axiovision digital camera system. Statistical analysis was performed using Student's t test unless indicated otherwise with a significance level of $p < .05$.

Mathematical Data Analysis

Using Matlab (version 7.12.0.635), the data were preconditioned by rotating the tracked data such that the fiber lay horizontally. This was done by extracting two coordinates, (x_1, y_1) and (x_2, y_2), along the straight fiber between the extreme points of cell motion. From this, we extracted the angle, the fiber made with x-axis, θ_f, through

$$\tan\ \theta_f = \frac{y_2 - y_1}{x_2 - x_1}. \quad (1)$$

The Cartesian form of the tracked points is $(x(t), y(t))$, where $x(t)$ and $y(t)$ are the x and y components of the cell's position at time t, respectively. The Cartesian form was then converted to its polar form, $z(t) = r(t)\ \exp(I\theta(t))$, where $r(t) = \sqrt{x(t)^2 + y(t)^2}$ and $\tan(\theta(t)) = y(t)/x(t)$. The tracked cell coordinates were rotated by applying the transformation $z^*(t) = x(t)\ \exp(-I\theta_f) = r(t)\ \exp(I\theta^*)$ and converted back to the Cartesian form, $(x^*(t) = r(t)\ \cos(\theta^*),\ y^*(t) = r(t)\ \sin(\theta^*))$. The new $x^*(t)$ and $y^*(t)$ coordinates of the satellite cells' positions were normalized to start from zero at the initial time point, producing trajectory data $x_0^*(t)$ and $y_0^*(t)$. In order to compare the trajectory data with a diffusive model of movement, we approximate the fiber with a cylinder that is infinitely long in the x-direction and has constant radius $r = 50$ μm (Supporting Information Fig. 1A).

Since the fiber is assumed to be unbounded, the mean square displacement (MSD) along the x-direction of a diffusing particle can be related to the diffusion coefficient, D_∞, and time, t, through the linear relation [21]

$$\langle x^2 \rangle = \frac{1}{N}\sum_i x_{i0}^*(t)^2 = 2D_x t, \quad (2)$$

where the summation occurs over all tracks, t, at a given time point, t, and N is the total number of tracks. Thus, we are able to characterize the motion along the fiber as diffusive if the MSD of the processed x data lies along a straight line. The diffusion coefficient can be derived from the gradient of this line.

However, this can only be used to characterize the x data. Across the fiber, in the y-direction, the movement of the cell on the surface of the fiber is bounded by the radius of the fiber. To produce a similar relation relating the MSD in the y-direction and the corresponding diffusion coefficient, D_y, we must take into account that the cell moves along a curved cylinder and we are projecting this motion onto the flat, one-dimensional y-axis. Note that, since the fiber is translucent, we are able to see the cell as it travels from back to front or front to back. Thus, instead of modeling the motion of the cell around the entire fiber, we are able to restrict the cell's motion to a semicircle with reflective boundary conditions (Supporting Information Fig. 1B).

Using this idealized setup, we consider a particle diffusing along a semicircle with constant diffusion coefficient, D_y, the evolution equation of the probability of the particle, $P(\omega,\omega_0,t)$, making an angle ω to the center of the circle at a time t given that the particle started at an angle ω_0 can be shown to take the form of an axisymmetric diffusion equation in polar coordinates [22],

$$\frac{\partial p}{\partial t} = \frac{D_y}{r^2}\frac{\partial^2 p}{\partial \omega^2}, \quad (3)$$

where the reflective boundaries are given by

$$\frac{\partial p}{\partial \omega}(\omega, \omega_0, t) = 0 \text{ at } \omega = 0 \text{ and } \pi \text{ rads}. \quad (4)$$

Finally, we need to specify an initial condition. Since we are unable to control the initial angle ω_0, we assume that the blebbing cells are uniformly placed across the surface of the cylinder at the beginning of the tracked data. Thus, to begin with, we give the cell an arbitrary but known initial angle $\omega = \omega_0$. Whence, the initial condition is $P(\omega,0) = \delta(\omega - \omega_0)/r$, where $\delta(\omega - \omega_0)$ is a delta function. Essentially, the delta function is zero everywhere except at $\omega_0 \in [0,\pi]$ and its integral over the interval $[0,\pi]$ is one [23]. The factor of r in the initial condition is needed to correct for the cylindrical polar coordinate transformation (Supporting Information Fig. 1C).

can be solved using a separable solution of Fourier modes [24]. Hence, we derive the solution:

$$P(\omega, \omega_0, t) = \frac{1}{r\pi} + \frac{2}{r\pi}\sum_{m=1}^{\infty} \cos(m\omega)\cos(m\omega_0) \times \exp\left(-D_y t\left(\frac{m}{r}\right)^2\right). \quad (5)$$

.The MSD is, thus, given by

$$\left\langle (y - y_0)^2 \right\rangle = \int_0^\pi (r\ \cos(\omega) - r\ \cos(\omega_0))^2 P(\omega, \omega_0, t) r\ \mathrm{d}\omega. \quad (6)$$

However, this is still conditioned on the initial point being $y = y_0$ when $\omega = \omega_0$. Thus, we average this MSD over the semicircle,

$$\langle y^2 \rangle = \frac{1}{r\pi}\int_0^\pi \int_0^\pi (r\ \cos(\omega) - r\ \cos(\omega_0))^2 P(\omega, \omega_0, t) r^2\ \mathrm{d}\omega\ \mathrm{d}\omega_0. \quad (7)$$

All of these integrals can be done analytically, allowing us to derive

$$\langle y^2 \rangle = r^2\left(1 - \exp\left(-\frac{D_y t}{r^2}\right)\right). \quad (8)$$

Rearranging shows that the diffusion coefficient, D_0, and the MSD of y can be related by,

$$\log\left(1 - \frac{\langle y^2 \rangle}{r^2}\right) = -\frac{D_y t}{r^2}. \quad (9)$$

Hence, if the data, when transformed as in, lies along a straight line with negative slope, then this suggests that the motion along the y direction is also diffusive. The diffusion coefficient can then be calculated from the gradient.

Results

Activation and Emergence Is Delayed in Aged Satellite Cells

Satellite cells are maintained in a quiescent state in undamaged muscle. Upon injury, they undergo activation resulting in a significant change in their molecular profile including the induction of MyoD expression. Isolation of single fibers from whole muscle mimics processes associated with muscle damage [16, 19, 20]. In the first set of experiments, we examined the behavior of aged satellite cells immediately after single fiber isolation. We found that the activation of satellite cells from aged fibers was significantly delayed compared to those found on fibers from young mice. Profiling of satellite cells showed that more than 96% of young satellite cells had initiated the expression of MyoD 8 hours after single muscle fiber isolation. In contrast, a significantly lower number of old satellite cells (88%) expressed MyoD expression after the same time period (49 young, 41 old fibers examined, $p < .001$, Fig. 1A).

We investigated whether the lag in activation of aged satellite cells delayed the emergence of satellite cells from their original sub-basal position. Single muscle fibers were isolated and cultured for differing periods of time and then fixed prior to immunohistological examination for position of the satellite cell (determined by Pax7 expression) in relation to the basal lamina (indicated by laminin expression). We found that after 15 hours culture, the first satellite cells on young fibers had taken a suprabasal position (Fig. 1B, 1C). Significantly, at the same time point, we were unable to detect any satellite cells in a similar position on aged muscle fibers (32 young, 30 old fibers examined, $p < .001$; Fig. 1B, 1D). Indeed, there was a 3-hour delay for the emergence of aged satellite cells, although there were significantly more satellite cells on the surface of the fiber from the young animals compared to the old (26 young and 23 old fibers examined, $p < .001$; Fig. 1B). Using SEM, we found that aged satellite cells remodeled the EMC to leave a scar on the surface of the muscle fiber and that the satellite cells displayed a smooth surface after emerging onto the myofiber, features also displayed by young satellite cells (Fig. 1E). The delay in emergence was transient, as an equal percentage of cells had assumed a suprabasal

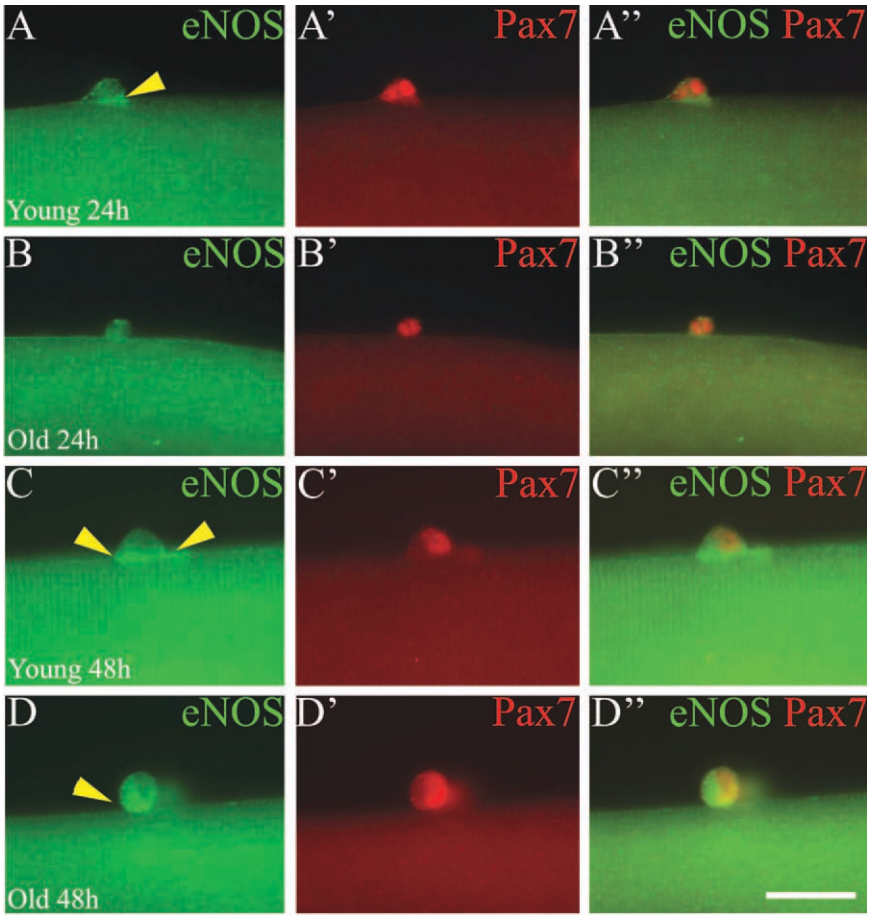

Figure 2. Delayed expression of eNOS in aged satellite cells compared to young satellite cells. **(A):** Cytoplasmic expression of eNOS in satellite cells on young fibers following 24 hours of culture (yellow arrowhead). **(A′):** Pax7 expression in eNOS expressing cell shown in (A). **(A″):** Cytoplasmic localization of eNOS (green) and nuclear expression of Pax7 (red) in young fiber satellite cells. **(B–B″):** Old fibers cultured for 24 hours display very little eNOS expression in satellite cells. **(C):** Young fibers cultured for 48 hours express eNOS located at the contact point between satellite cells and muscle fiber (yellow arrowheads). **(C′):** Pax7 expression in eNOS-expressing cell shown in (C). **(C″):** Cytoplasmic localization of eNOS (green) and nuclear expression of Pax7 (red) in young satellite cells. **(D):** Old fibers cultured for 48 hours express eNOS located at the contact point between satellite cells and muscle fiber (yellow arrowheads). **(D′):** Pax7 expression in eNOS expressing cell shown in (D). **(D″):** Cytoplasmic localization of eNOS (green) and nuclear expression of Pax7 (red) in satellite cells on old muscle fibers. Scale bar = 10 μm.

position 24 hours after single fiber isolation (30 young and 26 old fibers examined, $p > .05$; Fig. 1B). We have previously shown that activated satellite cells express eNOS, an enzyme responsible for the production of the potent signaling molecule NO [15]. We compared the abundance of eNOS in satellite cells on young and old fibers at different times after muscle dispersal. We found that satellite cells on young fibers cultured for 24 hours expressed eNOS in the cytoplasm (Fig. 2A–2A″). In contrast, similarly treated old fibers displayed very little eNOS in the satellite cells (Fig. 2B–2B″). However, after 48 hours, satellite cells on both old and young fibers displayed abundant levels of eNOS in the cytoplasm (Fig. 2C–2D″). These experiments therefore showed that activation, emergence, and expression of important signaling-associated proteins, three early key phases in the regeneration process, are delayed in aged muscle.

Proliferation Defects in Satellite Cells from Aged Muscle Fibers

We compared the proliferation and differentiation characteristics of young and aged satellite cells. The number of satellite cells on young fibers was significantly greater than on aged fibers (6.9 young, 4.7 old, 41 young, and 36 old fibers examined, $p < .001$, Fig. 3A). The number of satellite cells had more than doubled following the culture of young fibers for a period of 48 hours. In contrast, the number of satellite cells on aged fibers after an identical culture period had not increased compared to the number on freshly isolated 24 hours fibers and maintained the significant differences in cell number between the two cohorts (52 young and 48 old fibers examined, $p < .001$, Fig. 3A). In addition, the proliferation rate was also reduced in aged satellite cells, since we found that the number increased by 3.2-fold in aged fibers compared to a 3.8-fold increase in young fibers from a period of 48–72 hours (60 young and 50 old fibers examined, $p < .001$, Fig. 3A). Furthermore, we examined the localization of proliferating satellite cells by determining the size and number of clusters on young and aged fibers. Even though young satellite cells proliferated more rapidly compared to older cells, the number of cells per cluster was similar between the two groups at all time points examined (1.8 in young and 1.4 in old from an examination of 52 young and 48 old fibers at 48 hours and 4.2 in young and 3.6 in old from an examination of

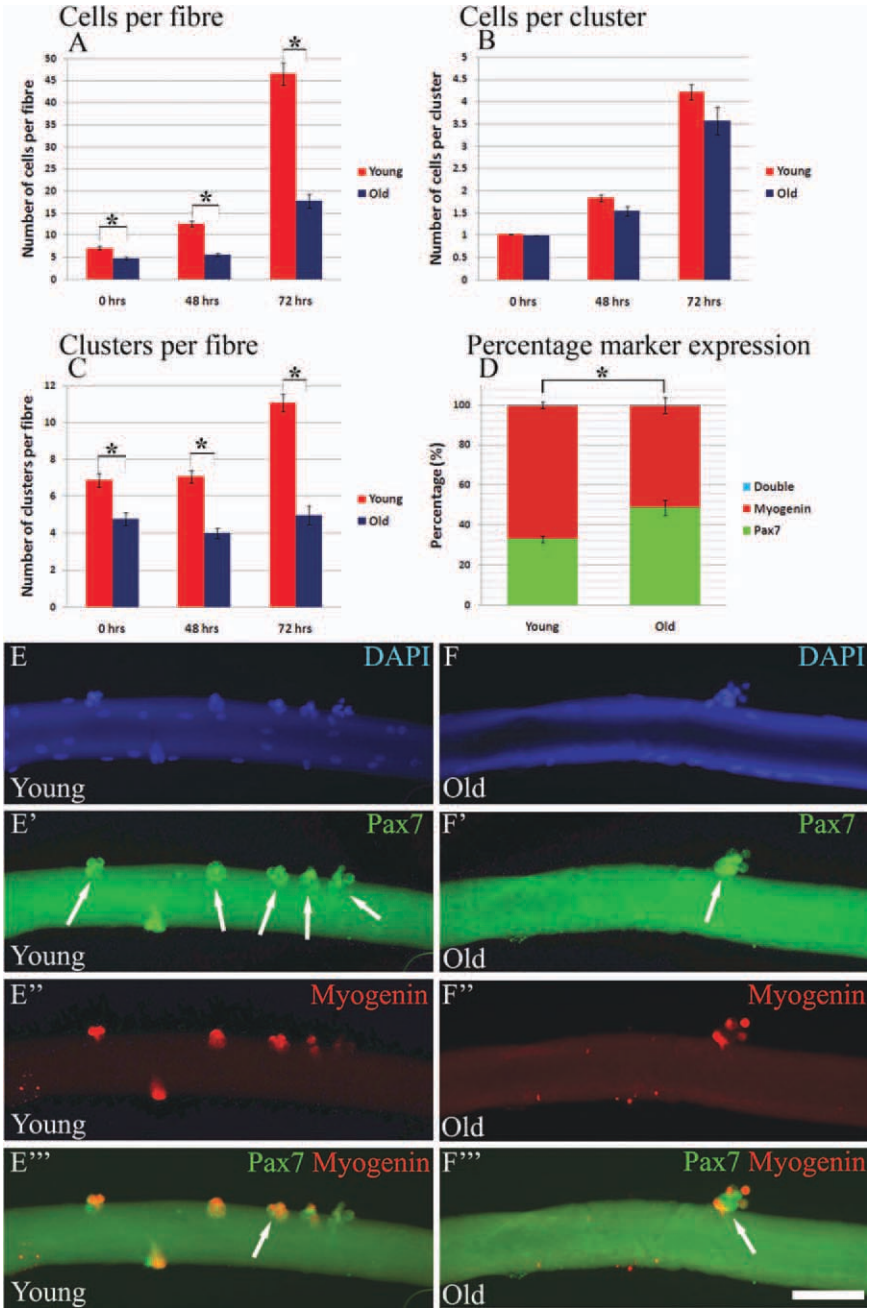

Figure 3. Aged satellite cells showed decreased rate of proliferation, decreased rate of cluster formation, and a delay in their differentiation program. **(A):** Young muscle fibers contained significantly more satellite cells identified through expression of Pax7 (6.9) than old muscle fibers (4.7) prior to culture (*, $p < .001$). Young fibers contained significantly more myoblasts, identified through expression of Pax7, compared to old fibers at 48 hours (*, $p < .001$). Likewise at 72 hours, young fibers significantly contained more committed (myogenin) and noncommitted cells compared to old fibers (*, $p < .001$). **(B):** The number of cells per cluster defined as the number of cells per grouping is not significantly different in cultured young and old muscle fibers. **(C):** The number of clusters per fiber is significantly greater on young fibers compared to the number of clusters on aged fibers at all time points examined (*, $p < .001$). **(D):** The number of myogenic precursors (expressing Pax7) on young fibers, 72 hours after culture, is significantly lower (33%) than those on aged muscle fibers (48.7%) (*, $p < .001$). The number of committed myogenic cells (expressing myogenin) on young fibers, 72 hours after culture, is significantly higher (66.9%) than those on aged muscle fibers (51%) (*, $p < .001$). **(E–F‴):** Muscle fibers cultured for 72 hours. (E): Young muscle fiber stained with DAPI. (E′): Young muscle fiber stained for Pax7 expression showing number of cell clusters (white arrows). (E″): Young muscle fiber stained for myogenin expression. (E‴): Young muscle fiber showing covisualization of Pax7 (green) and myogenin. Note that cluster is predominantly composed of myogenin-expressing cells. (F): Old muscle fiber stained with DAPI. (F′): Old muscle fiber stained for Pax7 expression showing sparse cell clusters (white arrow). (F″): Old muscle fiber stained for myogenin expression. (F‴): Old muscle fiber showing covisualization of Pax7 (green) and myogenin. Note that cluster is predominantly composed of Pax7-expressing cells. Scale bar = 50 μm. Abbreviation: DAPI, 4',6-diamidino-2-phenylindole.

60 young and 50 old fibers at 72 hours, $p > .05$, Fig. 3B). However, we found that the young satellite cells formed significantly more clusters compared to aged satellite cells (7.1 in young and 4.0 in old from an examination of 52 young and 48 old fibers at 48 hours and 11.1 in young and 4.9 in old from an examination of 60 young and 50 old fibers at 72

hours, $p < .001$, Fig. 3C, 3E–3F‴). Next, we examined the molecular profile of cells at 72 hours to determine the effect of ageing on the process of myogenic commitment to differentiation. Pax7 expression was used as an indicator of cells still in a precursor state, whereas expression of myogenin was taken as an indicator of cells committed to myogenic differentiation [20]. We found that the young fibers contained approximately 68% of cells expressing myogenin and 32% expressing Pax7. In contrast, aged fibers showed a distinct differentiation profile: there were significantly fewer myogenin-expressing cells and more Pax7-expressing cells (from a profile of 60 young and 50 old fibers at 72 hours, $p < .001$, Fig. 3D, 3E–3F‴). Therefore, aged satellite cells display a delay in their commitment to differentiation.

Finally, we examined the distribution of marker proteins associated with maintaining physical contact between satellite cells and the muscle fibers. To that end, we characterized the expression of the muscle-associated integrins-α6, -α7, and β1 in satellite cells on muscle fibers from young and old animals that had been cultured for 36 hours. A comparable relationship was established between the integrins and satellite cells from the two age groups in that the young satellite cells expressed higher levels of cell adhesion molecules compared to the levels displayed by old satellite cells (Fig. 4). This was particularly prominent in the expression of integrin α7 and β1 (Fig. 4C–4F″).

These results led us to investigate the expression of the integrins immediately after fiber isolation to gauge the nature of the stem cell niche occupied by satellite cells. We found that young satellite cells expressed integrin α6 at higher levels than cells on old fibers (Supporting Information Fig. 2A′–2B″). In contrast, young and old showed similar levels of integrin α7 expression (Supporting Information Fig. 2C′–2D″). Interestingly, we are unable to detect the expression of integrin β1 in either young or old satellite cells immediately after fiber isolation. These data suggest that the profile of satellite cell extracellular proteins changes during the activation process and may reflect the change in the environment experienced by the cells when they move away from their niche. These results show that ageing influences the profile of proteins functionally responsible for satellite cell-muscle fiber adhesion and migration.

Attenuated Migration Speeds, Bleb Number, and Bleb Dynamics in Aged Satellite Cells

The reduction in cluster number displayed by aged satellite cells could be explained by a defect in migration that reduces cluster splitting and separation. We examined migration characteristics directly using time-lapse microscopy and found that satellite cells from aged fibers migrated significantly slower (18.0 μm/hour from 12 tracked cells) than young satellite cells (40 μm/hour from 17 tracked cells, $p < .001$, Fig. 5A and Supporting Information Movie 1). We have previously shown that migrating satellite cells display dynamically extending and retracting membrane blebs [15]. We performed a detailed study to characterize blebbing on the surface of young and aged satellite cells. Quantification of bleb number revealed that young satellite cells displayed more than twice the number of blebs compared to aged satellite cells (27.4 blebs per cell on young satellite cells [$n = 12$] vs. 11.4 blebs per cell on old satellite cells [$n = 12$], $p < .001$, Fig. 5B, 5F, 5G). However, the average size of the blebs and shape (ratio of length/width) was similar between the two cohorts (0.084 μm for young satellite cells [$n = 9$] vs. 0.074 μm for old satellite cells [$n = 10$], $p > .05$, Fig. 5C, 5H). We performed a detailed analysis of bleb dynamics between the two ages and found that the life span of a bleb (comprising phases of bleb extension, maintenance, and retraction) was greater in aged cells (30.25 seconds for young satellite cells [$n = 16$] vs. 36.93 seconds for old satellite cells [$n = 60$], $p < .05$, Fig. 5D). Next, we investigated bleb dynamics by analyzing extension, stabilization, and retraction properties in young and aged cells. We found that there was a significant increase in the duration of bleb extension in aged cells (4.00 seconds for young satellite cells [$n = 16$] vs. 4.93 seconds for old satellite cells [$n = 60$], $p < .05$, Fig. 5E). On the other hand, stabilization time of aged cells compared to their younger counterparts was not significantly different (7.00 seconds for young satellite cells [$n = 16$] vs. 7.63 seconds for old satellite cells [$n = 60$], $p > .05$, Fig. 5E). However, there was a significant increase in the duration of time and it took aged satellite cells to retract the membrane extension compared to younger cells (19.25 seconds for young satellite cells [$n = 16$] vs. 24.37 seconds for old satellite cells [$n = 60$], $p < .05$, Fig. 5E). Despite the changes in the dynamics of the bleb life cycle with ageing, there was no significant change in the overall bleb shape in the two age cohorts as determined by examining the ratio of bleb length versus bleb diameter (Fig. 5H).

Mathematical Modeling of Young and Aged Satellite Cell Migration

We modeled the muscle fiber as a cylinder with infinite length and radius $r = 50$ μm. Blebbing cells are capable of moving along the fiber (x-axis) as well as along its curved surface. This curved surface was then projected on the flat plane allowing us to use the y-axis coordinates. Since the fiber is translucent and the cell can be tracked even if it travels behind the fiber, we model these boundaries as reflective (Supporting Information Fig. 1B, 1C). It is a standard result that for an unconstrained diffusion process, the MSD increases linearly in proportion to time. Hence, if it is possible to fit a straight line through the MSD in the x direction, then it can be said that the cells move in a manner consistent with Fickian diffusion. The gradient of this line can be used to find the diffusion coefficient for the movement, and an R^2 value can be found to give a measure of the goodness of fit (where $R^2 = 1$ indicates a perfect fit). This is not true for the bounded y-axis and in Methods, we have derived the corresponding relationship between the MSD in the y direction and the diffusion coefficient.

Analysis of movement of young cells along the length of the fibers (x-axis) gives an R^2 value of 0.903 at a gradient of 26.3 μm^2/minute, implying a diffusion rate of 13.2 μm^2/minute (Fig. 6A). These data indicate near diffusive movement along the fiber with relatively large movements during each time period. We found that the young cells also seem to move in a diffusive manner along the width of the fibers ($R^2 = 0.819$) but with smaller movements during each time period compared to those along the fiber (gradient $= -4.78 \times 10^{-4}$ μm^2/minute, diffusion rate $= 1.19$ μm^2/minute, Fig. 6B). A completely different profile was discovered following the analysis of aged satellite cell migration. The best fit curve for these data was a power-law plot, with MSD $= 1.45 \times 10^{-11} t^{5.62}$ (Fig. 6C), giving $R^2 = 0.983$. We were able to calculate an R^2 value of 0.663 for migration along the width of the fiber (y-axis) with a gradient of only -8.56×10^{-5} μm^2/minute, giving a diffusion rate of 0.214 μm^2/minute (Fig. 6D).

NO Rescues Migration Deficit of Aged Satellite Cells

We have previously shown that inhibition of NO production results in reduction in migration speeds of young satellite cells [15]. In this study, we found that aged satellite cells had

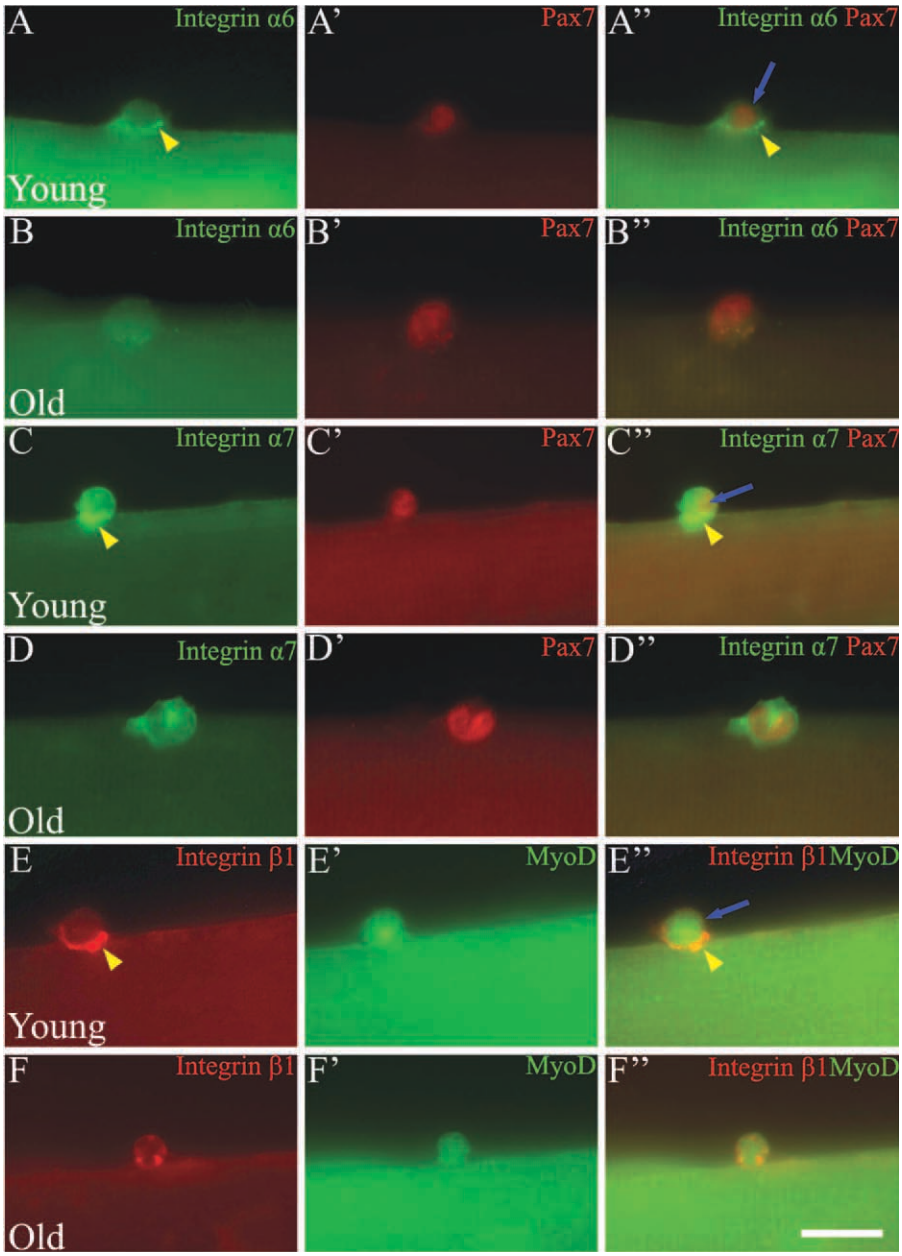

Figure 4. Profiling of integrin expression in young and old satellite cells during migration. **(A):** Expression of integrin α6 was present at the interface between young satellite cell and the muscle fiber that had been cultured for 36 hours (yellow arrowhead). **(A′):** Pax7 expression permits the identification of the satellite cell shown in (A). **(A″):** Covisualization of integrin α6 (yellow arrowhead) and Pax7 (blue arrow) in young satellite cell. **(B–B″):** Satellite cells from old muscles cultured for 36 hours expressed very little integrin α6. **(C):** Integrin α7 was detected between the satellite cells and muscle fiber in young muscle samples. **(C′):** Pax7 marks the position of satellite cells in sample shown in (C). **(C″):** Covisualization of integrin α7 (yellow arrowhead) and Pax7 (blue arrow) in young satellite cell. **(D–D″):** Satellite cells from old muscles cultured for 36 hours expressed less integrin α7 compared to young cells. **(E):** High levels of integrin β1 localized between the satellite cells and myofiber from young cultured muscle. **(E′):** MyoD marks the position of satellite cell shown in (E). **(E″):** Covisualization of integrin β1 (yellow arrowhead) and MyoD (blue arrow) in young satellite cell. **(F):** Punctate expression of integrin β1 in an old satellite cell. **(F′):** MyoD marks the position of satellite cell shown in (F′). **(F″):** Covisualization of integrin β1 and MyoD in an old satellite cell. Scale bar = 10 μm.

slower migration rates (18.0 μm/hour) compared to younger cells (40 μm/hour) (Fig. 5A), and therefore we investigated whether provision of NO could overcome this deficit. We isolated single fibers from aged muscle and supplemented the media with the potent NO donor (*Z*)-1-[*N*-(3-aminopropyl)-*N*-(*n*-propyl)amino]diazen-1-ium-1,2-diolate (also known as PAPA-NONOate, 100 μM). Addition of PAPA-NONOate resulted in aged satellite cells migrating at more than twice the speed and at rates comparable to young satellite cells (44.2 μm/hour from 20 tracks, $p < .001$; Fig. 5I and Supporting Information Movie 1). Therefore, addition of NO significantly reverses the deficit in migration speed displayed by aged satellite cells. Interestingly, addition of PAPA-NONOate to young muscle fibers had no significant effect on satellite cells migration speed (Fig. 5J).

We next examined the effect of PAPA-NONOate on the directionality of movement of aged satellite cells by calculating the MSD along and across the fiber. In contrast to the

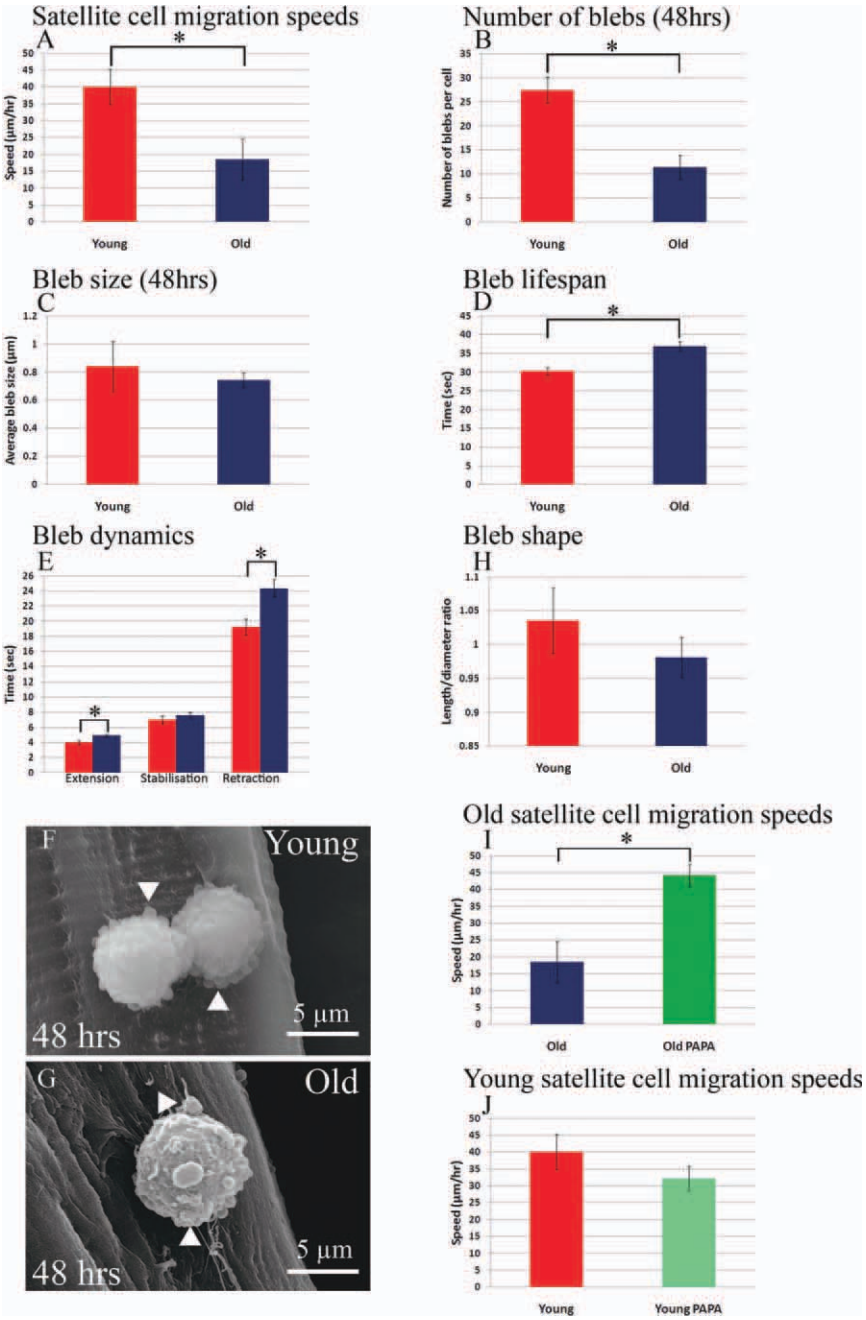

Figure 5. Aged satellite cells migrate slower and have abnormal bleb number and blebbing characteristics. **(A):** Satellite cells on young fibers move significantly faster (40 μm/hour from 17 tracked cells) compared to satellite cells on aged fibers (18.0 μm/hour from 12 tracked cell) (*, $p < .001$). **(B):** The number of blebs on young satellite cells following 48 hours of culture is significantly greater [26] than those on aged fibers [12] (*, $p < .001$). **(C):** The average maximum size of blebs on young and old satellite cells on fibers cultured for 48 hours did not differ significantly. **(D):** The total lifespan of a bleb was longer in aged satellite cells (36.9 seconds) found on muscle fibers that were cultured for 48 hours than those on similarly developed fibers from young animals (30.3 seconds; *, $p < .05$). **(E):** The increase in total bleb lifespan found in aged satellite cells was due to a significant increase in the extension (aged = 4.9 seconds, young = 4 seconds) and retraction (aged = 24.4 seconds, young = 19.3 seconds) periods (*, $p < .05$). **(F):** Scanning electron micrograph shows two satellite cells on the surface of young muscle fibers following 48 hours of culture displaying numerous blebs of similar size (arrowhead). **(G):** Scanning electron micrograph shows a satellite cell on the surface of an old muscle fiber following 48 hours of culture displaying a few blebs of varying size (arrowheads). **(H):** Bleb shape developed on satellite cells on fibers cultured for 48 hours calculated as the ratio of maximal length/diameter was not significantly different between young and aged muscles. **(I):** The low migration of aged satellite cells (18 μm/hour) is significantly increased following the introduction of 100 μM (Z)-1-[N-(3-aminopropyl)-N-(n-propyl)amino]diazen-1-ium-1,2-diolate-PAPA (44.2 μm/hour, 20 cells tracked; *, $p < .001$). **(J):** The migration speed of young satellite cells (40.0 μm/hour) is not significantly changed following the introduction of 100 μM (Z)-1-[N-(3-aminopropyl)-N-(n-propyl)amino]diazen-1-ium-1,2-diolate-PAPA (32.2 μm/hour, 22 cells tracked; $p > .05$).

nonlinear MSD profile of untreated aged satellite cells, the same cells treated with PAPA-NONOate displayed a linear profile ($R^2 = 0.901$) with a gradient of 24.2 μm^2/minute (Fig. 6E). PAPA-NONOate reduced the R^2 value for displacement along the width of the fiber although it increased the diffusion rate from 0.214 μm^2/minute to 4.31 μm^2/minute (Fig. 6F).

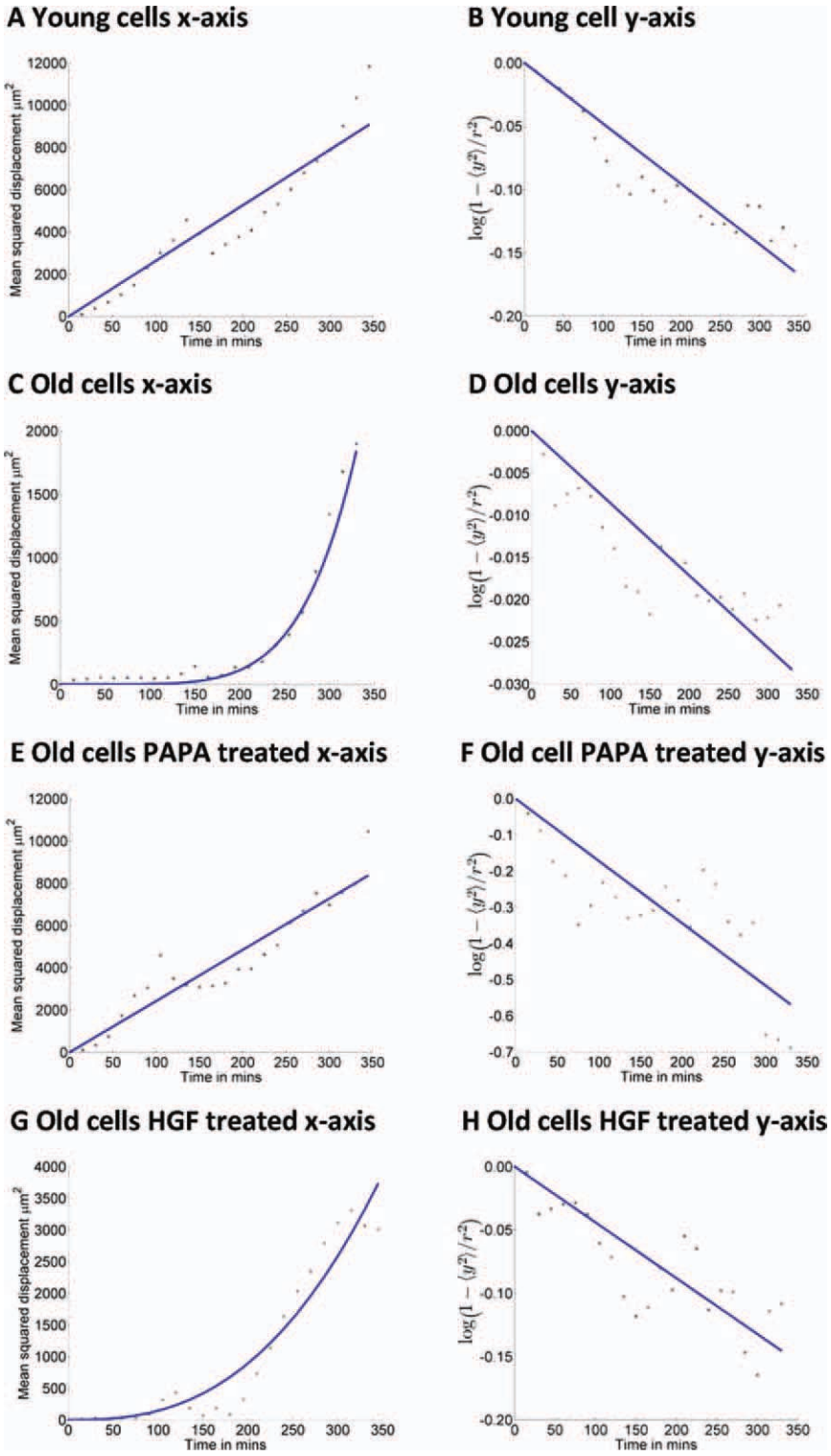

Figure 6. Characteristics of satellite cell motion. See Methods for more details. In each case, only the first 345 minutes of data were used. The dots denote the data points and the blue curve is the curve of best fit, which is linear in all images except **(C)** and **(G)**. **(A):** Mean square displacement (MSD) of young satellite cells along the *x*-axis. Since the points lie along an approximately straight line in both cases ($R^2 = 0.903$), this suggests that young satellite cells move diffusely along and across the fiber with diffusive rate constant $D_x = 13.1$ μm^2/minute. **(B):** Logarithmic transformed *y*-axis displacement data. The negative gradient ($R^2 = 0.819$) can be related back to the diffusion coefficient giving $D_y = 1.19$ μm^2/second. (C): MSD of old satellite cells along the *x*-axis. These points do not lie along a straight line, instead a power law (at^m) is fitted to the data ($R^2 = 0.981$, $m = 5.6$, $a = 1.45 \times 10^{-11}$). This suggests that the old cells are not diffusive along the *x*-axis. **(D):** Logarithmic transformed *y*-axis displacement data. The negative gradient ($R^2 = 0.663$) suggests that the particles are diffusive across the fiber with diffusion rate $D_y = 0.214$ μm^2/minute. **(E, F)** MSD and logarithmic transformed MSD of PAPA-treated old satellite cells along the *x*-axis and *y*-axis, respectively. Since the points lie along an approximately straight line ($R^2 = 0.901$ and 0.593, respectively), this suggests that old PAPA-treated satellite cells move diffusely along and across the fiber with diffusive rate constants $D_x = 12.1$ μm^2/minute and $D_y = 4.31$ μm^2/minute, respectively. (G): MSD of old satellite cells treated with HGF along the *x*-axis. These points do not lie along a straight line, instead a power law (at^m) is fitted to the data ($R^2 = 0.923$, $m = 2.63$, $a = 8.05 \times 10^{-4}$). This suggests that the old cells are not diffusive along the *x*-axis. **(H):** Logarithmic transformed *y*-axis displacement data for old satellite cells treated with HGF. The negative gradient ($R^2 = 0.667$) suggests that the particles are diffusive across the fiber with diffusion rate $D_y = 1.10$ μm^2/minute. Abbreviations: HGF, hepatocyte growth factor; PAPA, (Z)-1-[N-(3-aminopropyl)-N-(n-propyl)amino]diazen-1-ium-1,2-diolate.

Therefore, NO not only restores the speed of migration in aged satellite cells but also the diffusive characteristics displayed by young cells, particularly in the x direction, along the fiber.

HGF Restores Aged Satellite Cells Migration Speed but Not Directionality of Movement

HGF has been shown to promote satellite cell activation and has been proposed to induce migration [25, 26], and therefore has functional properties akin to those of NO. We carried out a suite of experiments to determine whether HGF mimicked the action of NO. We found that HGF was able to promote the activation of not only young but also old satellite cells in a concentration-dependent manner (Fig. 7A). We quantified the effect of supplementing culture medium with HGF on the emergence of satellite cells from the sublaminal position and found that it accelerated the rate at which cells assumed a suprabasal localization (Fig. 7B). A similar effect was induced on old muscle fibers by PAPA-NONOate (Fig. 7B). We next determined the effect of HGF on satellite cell migration speed. We found that HGF caused a significant increase in the rate of movement of old satellite cells (from 25.6 to 41.5 μm/hour; Fig. 7C) but had no significant effect on young satellite cell (Fig. 7D). Having found that HGF altered the rate of aged satellite cell movement, we next determined its effect on bleb development. Measurement of bleb dimensions revealed that HGF did not alter the size of blebs on old satellite cells (Fig. 7E). However, it induced a greater number of blebs (Fig. 7F, 7H, 7J). HGF had no significant effect on the size or number of blebs on young satellite cells (Fig. 7E–7G, 7I). Finally, we next determined the impact of HGF on the directionality of movement of aged satellite cells by calculating the MSD along and across the fiber. The best fit curve for these data was not a linear relationship but a power-law plot, with MSD $= at^m$ ($m = 2.63$, $a = 8.05 \times 10^{-4}$) (Fig. 6G), giving $R^2 = 0.923$. We were able to calculate an R^2 value of 0.667 for migration along the width of the fiber (y-axis) with a gradient of -4.407×10^{-4}/minute, giving a diffusion rate of 1.10 μm^2/minute (Fig. 6H). These results show that while HGF is able to accelerate the rate of aged satellite cell activation, emergence, number of blebs, and migration speed, it does not re-establish the memoryless character of satellite cell movement along the fiber displayed by young cells.

Discussion

Sarcopenia is defined as the degenerative loss of skeletal muscle mass and strength associated with the ageing process. Previous work has shown that skeletal muscle undergoes numerous changes with age including: reduction in myofiber cross-sectional area [3]; a shift toward an oxidative metabolic profile [4]; an increase in mitochondrial proliferation and accumulation of mitochondrial mutations [6, 27]; an increase in interstitial connective tissue deposition [5]; a decrease in satellite cell number; and a decrease in the efficiency of skeletal muscle regeneration [8, 28]. Results from this study extend the list of age-related changes in skeletal muscle to include a reduction in satellite cell migration speed and altered mechanism of migration along the muscle fiber. We have previously shown that in the single-fiber culture model, satellite cells become activated after the dispersal process and then remodel the basal lamina to develop an opening through which they move to assume a position on the surface of the myofibers [15]. In this study, we found that both the time of activation and time for the satellite cells to assume a suprabasal laminal position were delayed in aged muscle. The delay in activation may be explained by the differing levels of satellite cell quiescence in the two age groups. Although satellite cells at both time points are in a mitotically arrested state, it has been previously shown that young muscle stem cells exist at a more metabolically active level than older muscle stem cells (in particular for processes required for protein synthesis and protein folding) compared to older cells [29]. Therefore, the delay in the activation of aged satellite cells could be due to the increase in time required for the translation of proteins used as markers associated with this process. We suggest that the activation process of old satellite cells is hindered not only by greater metabolic inactivity but also potentially by the age-related development of the basal lamina between the stem cells and the myofiber [29]. We propose that a basal lamina between the satellite cell and myofiber would impede the diffusion of activation signals that arise from the myofiber.

In addition, the delay in the emergence period highlights changes in the extracellular environment that take place in muscle during ageing. It is well documented that ageing leads to an increase in the thickness of the endomysium on top of the satellite cell, and therefore it would be a greater challenge for cells to create an opening through which to emerge [5].

The key finding of our study is the reduced migration speed of aged satellite cells along the muscle fiber. We found that the young cells move at twice the rate of old cells (40 μm/hour vs. 18.5 μm/hour). It is important to point out that both sets of fibers were treated in an identical manner during their preparation and cultured in the same medium. Therefore, the difference in migration speed indicates the existence of an inherent difference between young and old satellite cells with regards to movement. It is generally accepted that adhesions need to be established between a cell and its substratum in order to generate traction forces required for movement. Integrins are a large family of heterodimeric glycoproteins that serve as cell-extracellular matrix adhesion molecules [30]. Previous work has shown that embryonic and adult skeletal muscles express integrin $\alpha 6\beta 1$ and $\alpha 7\beta 1$ both of which have a high affinity for laminin, a major constituent of muscle fiber basal lamina [31]. We have found a reduction in the expression of the three major muscle integrin components in aged satellite cells. These results suggest that altered integrin expression by satellite cells is a feature of ageing that could impact on migration. This notion is supported by elegant work performed by Siegel et al. who showed that the deployment of neutralizing antibodies directed against integrins $\alpha 7$ or $\beta 1$ significantly decreased the speed of primary satellite cells [16].

The high migration speeds displayed by young satellite cells can be attributed to the blebbing mechanism that is used for migration [18]. Importantly, our time lapse studies showed that even though old satellites move at relatively low speed, they undergo blebbing and do not revert to the slower lamellipodia-based migration mechanism. It is worth highlighting that rate of satellite cell movement does not seem to be related to myogenic differentiation. We have previously shown that the early onset of differentiation in satellite cells (signified by myogenin expression) is not accompanied by a significant change in migration speed [15]. This point is further accentuated by the findings in this study that show that aged satellite cells have a delay in their myogenic differentiation program yet move slower than young cells that are further down their commitment program. However, the dynamics of blebbing between the two age groups differ significantly and this rather than the differentiation status seems to be a major factor in controlling migration speeds. We found that the size of blebs between the two cohorts is similar but there were significant differences in the number of blebs as well as the time taken for bleb extension and retraction. These results

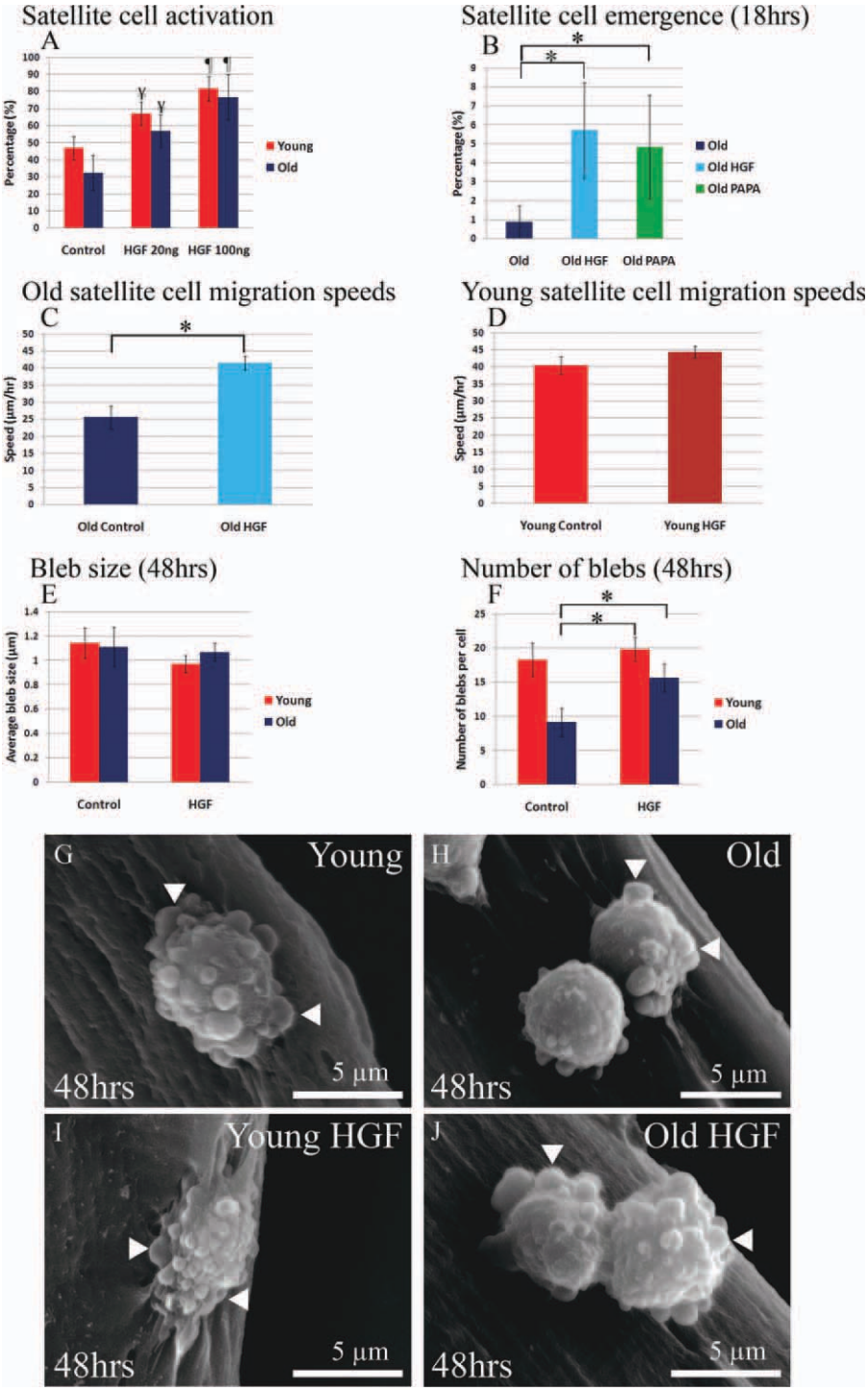

Figure 7. HGF accelerates activation, emergence, and speed of migration of aged satellite cells. **(A):** Activation of satellite cells, gauged by expression of MyoD, was quantified at 3 hours after fiber dispersal in the presence of HGF. Twenty nanograms per milliliter and 100 ng/ml HGF induced greater activation of both old and young cells (*, $p < .05$). Only significance for old cells is shown for the easy of graphic representation. **(B):** Emergence gauged by the suprabasal lamina position of Pax7 expressing aged satellite cells 18 hours after fiber dispersal was accelerated by 20 ng/ml HGF and 100 μM PAPA (*, $p < .05$). **(C):** Satellite cells on old fibers treated with 20 ng/ml HGF move significantly faster (41.5 μm/hour from 15 tracked cells) compared to untreated satellite cells on aged fibers (25.6 μm/hour from 15 tracked cells) (*, $p < .05$). **(D):** Satellite cells on young fibers treated with 20 ng/ml HGF did not move significantly faster (44.4 μm/hour from four tracked cells) compared to untreated satellite cells on young fibers (40.5 μm/hour from 22 tracked cells) (*, $p > .05$). **(E):** The average maximum size of blebs on young and old satellite cells on fibers cultured for 48 hours and treated with 20 ng/ml HGF did not differ significantly from untreated cells. **(F):** The number of blebs on aged satellite cells following 48 hours of culture in the presence of 20 ng/ml HGF is significantly greater (15.7) than those on untreated aged fibers (9.2) (*, $p < .05$). **(G):** Scanning electron micrograph of young untreated satellite cell decorated with blebs (arrowheads). **(H):** Scanning electron micrograph of old untreated satellite cell showing fewer blebs (arrowheads) compared to untreated young cell in G. **(I):** Scanning electron micrograph of young 20 ng/ml HGF-treated satellite cell decorated with blebs (arrowheads). **(J):** Scanning electron micrograph of old 20 ng/ml HGF-treated satellite cell decorated with blebs (arrowheads). Abbreviations: HGF, hepatocyte growth factor; PAPA, (Z)-1-[N-(3-aminopropyl)-N-(n-propyl)amino]diazen-1-ium-1,2-diolate.

give an insight into the importance of features of blebbing in relation to movement suggesting that the number of blebs and their rapid extension and retraction support high migration speeds. This conclusion is supported by the data from the two manipulations of old satellite cells that increased the migration speed of aged satellite cells; both PAPA-NONOate and HGF treatments resulted in an increase in the number. Importantly, these parameters can be manipulated by altering properties of the cytoskeleton and future work will examine the significance of each particular feature of blebbing on the migration speed of satellite cells [32].

Mathematical analysis of the migration trajectories of satellite cells revealed a number of important features. We showed that young satellite cells move in a diffusive manner both along and across the fiber. This suggests that the blebbing cells undergo a "memoryless" random walk with equal probability of moving left or right at each time point. Additionally, data analysis of the gradients from the MSD over time plots implies that young satellite cells take bigger steps along the fiber than across its width in a given time frame. In contrast, aged satellite cells appear to move along the fiber in a superdiffusive manner, so that the MSD is higher than a linear dependence on time would suggest. This indicates a more active movement than the usual Fickian diffusion and is most often associated with directed active transport processes [33].

NO is a potent regulator of migration in numerous cell types [34–36]. Here, we showed that the speed deficit and migration anomalies of aged satellite cells can be reversed through the action of NO donors. These results are consistent with our previous finding that showed that small compound inhibitors of NO production decreased the rate of satellite cell migration [15]. These results imply that inherent age-related changes in the myofiber and satellite cells can be overcome, at least as far as migration is concerned by delivering NO.

In addition, our work reveals that migration is a multifaceted mechanism and involves parameters other than speed of movement. We have shown that aged satellite cells treated with HGF respond by increasing their rate of movement to levels displayed by young cells. However, HGF did not correct the Fickian diffusion characteristics of aged satellite cells. Previous work has shown in the context of satellite cell activation that NO acts upstream of HGF [26]. Our data are congruent with this relationship. We suggest that NO promotes the rate of satellite cell activation and movement possible via HGF but also another important property, direction of movement, but that this process is independent of HGF-mediated signaling. We are currently dissecting the divergence of NO-mediated signaling from HGF action to gain a comprehensive understanding of the role played by these molecules in controlling satellite cell behavior.

We have shown that aged satellite cells move more slowly compared to young cells and by a different mechanism. One simple hypothesis encompassing our major finding is that NO production is decreased during ageing. When such a deficit exists, we do not know whether it is due to compromised NO production by the myofibers and/or satellite cells as both are capable of its production [15, 37]. The evidence for decreased age-related NO activity in muscle is controversial with some studies showing such a trend, whereas others propose that NO levels actually increase [38, 39]. Nevertheless, there is an extensive body of work that shows that NO promotes skeletal muscle repair, a process attributed to satellite cell activation [40]. We have shown that the activation of eNOS expression by aged satellite cells is delayed following fiber dispersal. We propose that the lag in NO production by aged satellite cells could be as detrimental to the regenerative process as not producing it in the first place by accepting that robust regeneration occurs only during a narrow time window limited by the action of other often antagonistic cellular events, for example, macrophage infiltration and fibrosis [41]. In our experiments, we introduced the NO donor after the activation period, when cells were moving on the surface of the fiber, and therefore we believe that this signaling molecule plays roles at multiple stages during regeneration. NO production can be increased by a number of well-characterized drugs. For example, the synthesis of NO from NO synthases (NOS) can be stimulated through the addition of L-arginine [42] (the main substrate for NOS) and through the use of growth factors such as epidermal growth factor, which act to increase NO production through the Akt-mediated phosphorylation of eNOS [43] or through increased transcription of iNOS [44]. In addition to simply increasing NO synthesis, other therapeutic options include the ability to modulate downstream NO signaling to improve satellite cell migration in older muscle. Treatment with phosphodiesterase type 5 inhibitors, which are routinely used clinically, is known to increase the persistence of cGMP signalling, thus amplifying endogenous NO signaling [45]. Importantly, a number of these treatments have undergone efficacy and safety trials in humans and are routinely prescribed. In future work, we will examine whether drugs that promote NO production or modulate NO signaling improve the regeneration of aged muscle.

Future work will determine whether ageing affects the movement of human satellite cells in a manner discovered in this study in mice. More immediately, we will investigate whether activation of the NO signaling pathway in whole muscle can overcome the age-related increase in regeneration time through its ability to promote satellite cell migration in animal models.

Conclusion

Our studies show that aged skeletal muscle stem cells (satellite cells) migrate considerably slower than their young counterparts. The migration deficit displayed by aged cells is due to them displaying fewer blebs and having reduced dynamic nature of the blebbing process. Aged satellite cells also display an altered mechanism of movement compared to young cells. Finally we show that age associated changes displayed by migrating satellite cells can be eliminated by nitric oxide.

Acknowledgments

We are grateful to the BBSRC (BB/E52881X-1), Natural Biosciences, and Systems Biology Laboratory (SBL) for generous funding that has enabled this work to be performed. In particular, we are grateful to Dr. Steve Ray of Natural Biosciences and Dr. Mike Fischer of SBL for their continued support for academic-based research focusing on improving human health. We thank Drs. S. Jaffer and M. Tindall for assistance in the preparation of this work. P.K.M. was partially supported by a Royal Society Wolfson Research Merit Award. T.E.W. and L.D. thank the EPSRC for support. P.R.D. thanks the British Heart Foundation (Grant FS/08/056) for support. We also thank Dr. Silvia Torelli, Dr. Francesco Conti, and Professor Uli Mayer for providing information and antibodies for integrin profiling of satellite cells. We are also indebted to two anonymous reviewers for providing constructive criticism and making valuable suggestions that have resulted in an improved manuscript.

Disclosure of Potential Conflicts of Interest

The authors indicate no potential conflicts of interest.

REFERENCES

1 Cruz-Jentoft AJ, Baeyens JP, Bauer JM et al. Sarcopenia: European consensus on definition and diagnosis: Report of the European Working Group on sarcopenia in older people. Age Ageing 2010;39:412–423.
2 Berger MJ, Doherty TJ. Sarcopenia: Prevalence, mechanisms, and functional consequences. Interdiscip Top Gerontol 2010;37:94–114.
3 Faulkner JA, Brooks SV, Zerba E. Muscle atrophy and weakness with aging: Contraction-induced injury as an underlying mechanism. J Gerontol A Biol Sci Med Sci 1995;50 Spec No:124–129.
4 Alnaqeeb MA, Goldspink G. Changes in fibre type, number and diameter in developing and ageing skeletal muscle. J Anat 1987;153:31–45.
5 Marshall PA, Williams PE, Goldspink G. Accumulation of collagen and altered fiber-type ratios as indicators of abnormal muscle gene expression in the mdx dystrophic mouse. Muscle Nerve 1989;12: 528–537.
6 Aiken J, Bua E, Cao Z et al. Mitochondrial DNA deletion mutations and sarcopenia. Ann N Y Acad Sci 2002;959:412–423.
7 Radak Z, Chung HY, Goto S. Systemic adaptation to oxidative challenge induced by regular exercise. Free Radic Biol Med 2008;44: 153–159.
8 Gutmann E, Carlson BM. Regeneration and transplantation of muscles in old rats and between young and old rats. Life Sci 1976;18: 109–114.
9 Schultz E, Lipton BH. Skeletal muscle satellite cells: Changes in proliferation potential as a function of age. Mech Ageing Dev 1982;20: 377–383.
10 Ishido M, Kasuga N. In situ real-time imaging of the satellite cells in rat intact and injured soleus muscles using quantum dots. Histochem Cell Biol 2011;135:21–26.
11 Wang W, Pan H, Murray K et al. Matrix metalloproteinase-1 promotes muscle cell migration and differentiation. Am J Pathol 2009; 174:541–549.
12 Lafreniere JF, Mills P, Tremblay JP et al. Growth factors improve the in vivo migration of human skeletal myoblasts by modulating their endogenous proteolytic activity. Transplantation 2004;77:1741–1747.
13 Satoh A, Huard J, Labrecque C et al. Use of fluorescent latex microspheres (FLMs) to follow the fate of transplanted myoblasts. J Histochem Cytochem 1993;41:1579–1582.
14 Peault B, Rudnicki M, Torrente Y et al. Stem and progenitor cells in skeletal muscle development, maintenance, and therapy. Mol Ther 2007;15:867–877.
15 Otto A, Collins-Hooper H, Patel A et al. Adult skeletal muscle stem cell migration is mediated by a blebbing/amoeboid mechanism. Rejuvenation Res 2011;14:249–260.
16 Siegel AL, Atchison K, Fisher KE et al. 3D timelapse analysis of muscle satellite cell motility. Stem Cells 2009;27:2527–2538.
17 Charras GT, Yarrow JC, Horton MA et al. Non-equilibration of hydrostatic pressure in blebbing cells. Nature 2005;435:365–369.
18 Charras G, Paluch E. Blebs lead the way: How to migrate without lamellipodia. Nat Rev Mol Cell Biol 2008;9:730–736.
19 Otto A, Schmidt C, Luke G et al. Canonical Wnt signalling induces satellite-cell proliferation during adult skeletal muscle regeneration. J Cell Sci 2008;121:2939–2950.
20 Zammit PS, Golding JP, Nagata Y et al. Muscle satellite cells adopt divergent fates: A mechanism for self-renewal? J Cell Biol 2004;166: 347–357.
21 Kärger J. Straightforward derivation of the long-time limit of the mean-square displacement in one-dimensional diffusion. Phys Rev A 1992;45:4173.
22 van Kampen NG. Stochastic Processes in Physics and Chemistry. Amsterdam: North Holland, 2007.
23 Collins RE. Mathematical Methods for Physicists and Engineers. Mineola: Dover Publications, 1999.
24 Kreyszig E. Advanced Engineering Mathematics. New Delhi: Wiley-India, 2007.
25 Tatsumi R, Sheehan SM, Iwasaki H et al. Mechanical stretch induces activation of skeletal muscle satellite cells in vitro. Exp Cell Res 2001;267:107–114.
26 Anderson J, Pilipowicz O. Activation of muscle satellite cells in single-fiber cultures. Nitric Oxide 2002;7:36–41.
27 Bua EA, McKiernan SH, Wanagat J et al. Mitochondrial abnormalities are more frequent in muscles undergoing sarcopenia. J Appl Physiol 2002;92:2617–2624.
28 Shefer G, Van de Mark DP, Richardson JB et al. Satellite-cell pool size does matter: Defining the myogenic potency of aging skeletal muscle. Dev Biol 2006;294:50–66.
29 Snow MH. The effects of aging on satellite cells in skeletal muscles of mice and rats. Cell Tissue Res 1977;185:399–408.
30 Spence HJ, Chen YJ, Winder SJ. Muscular dystrophies, the cytoskeleton and cell adhesion. Bioessays 2002;24:542–552.
31 Mayer U. Integrins: Redundant or important players in skeletal muscle? J Biol Chem 2003;278:14587–14590.
32 Hagmann J, Burger MM, Dagan D. Regulation of plasma membrane blebbing by the cytoskeleton. J Cell Biochem 1999;73:488–499.
33 Kumar N, Harbola U, Lindenberg K. Memory-induced anomalous dynamics: Emergence of diffusion, subdiffusion, and superdiffusion from a single random walk model. Phys Rev E 2010;82:021101.
34 Cartwright JE, Tse WK, Whitley GS. Hepatocyte growth factor induced human trophoblast motility involves phosphatidylinositol-3-kinase, mitogen-activated protein kinase, and inducible nitric oxide synthase. Exp Cell Res 2002;279:219–226.
35 Kawasaki K, Smith RS Jr., Hsieh CM et al. Activation of the phosphatidylinositol 3-kinase/protein kinase Akt pathway mediates nitric oxide-induced endothelial cell migration and angiogenesis. Mol Cell Biol 2003;23:5726–5737.
36 Noiri E, Peresleni T, Srivastava N et al. Nitric oxide is necessary for a switch from stationary to locomoting phenotype in epithelial cells. Am J Physiol 1996;270:C794–C802.
37 Planitzer G, Baum O, Gossrau R. Skeletal muscle fibres show NADPH diaphorase activity associated with mitochondria, the sarcoplasmic reticulum and the NOS-1-containing sarcolemma. Histochem J 2000;32:303–312.
38 Richmonds CR, Boonyapisit K, Kusner LL et al. Nitric oxide synthase in aging rat skeletal muscle. Mech Ageing Dev 1999;109:177–189.
39 Capanni C, Squarzoni S, Petrini S et al. Increase of neuronal nitric oxide synthase in rat skeletal muscle during ageing. Biochem Biophys Res Commun 1998;245:216–219.
40 Filippin LI, Cuevas MJ, Lima E et al. Nitric oxide regulates the repair of injured skeletal muscle. Nitric Oxide 2011;24:43–49.
41 Grounds MD, Davies MJ. Chemotaxis in myogenesis. Basic Appl Myol 1996;6:469–483.
42 Tsao PS, McEvoy LM, Drexler H et al. Enhanced endothelial adhesiveness in hypercholesterolemia is attenuated by L-arginine. Circulation 1994;89:2176–2182.
43 Makondo K, Kimura K, Kitamura N et al. Hepatocyte growth factor activates endothelial nitric oxide synthase by Ca(2+)- and phosphoinositide 3-kinase/Akt-dependent phosphorylation in aortic endothelial cells. Biochem J 2003;374:63–69.
44 Dash PR, Whitley GS, Ayling LJ et al. Trophoblast apoptosis is inhibited by hepatocyte growth factor through the Akt and beta-catenin mediated up-regulation of inducible nitric oxide synthase. Cell Signal 2005;17:571–580.
45 Montani D, Chaumais MC, Savale L et al. Phosphodiesterase type 5 inhibitors in pulmonary arterial hypertension. Adv Ther 2009;26: 813–825.

See www.StemCells.com for supporting information available online.